1.8 THE TURBULENCE STRUCTURE OF THE STABLE ATMOSPHERIC BOUNDARY LAYER AROUND A COASTAL HEADLAND: I. AIRCRAFT OBSERVATIONS

Ian M. Brooks*
Scripps Institution of Oceanography, La Jolla, California

Stefan Söderberg and Michael Tjernström
Stockholm University, Stockholm, Sweden

1. INTRODUCTION

The coastal zone is inherently complex, displaying a high degree of spatial and temporal variability forced by the contrast in surface conditions between land and sea, and the restrictions on the flow of both atmosphere and ocean imposed by coastal topography and bathymetry. This complexity presents a significant challenge to our ability to predict coastal weather. The situation is compounded by the frequent occurrence of stable conditions in many coastal locations. The stable boundary layer (BL) is much less well understood than the convective case, due in part to the difficulty of making high quality measurements in conditions of low intensity, and sometimes intermittent, turbulence. The parameterizations of surface fluxes are largely unverified for stable conditions over the oceans; consequently numerical models often perform poorly (Nappo and Bach, 1997).

Stable conditions are a widespread and persistent feature off the coast of northern California and Oregon during the summer months, resulting from the predominantly northwesterly wind, which advects a marine air mass from the open ocean over the cold upwelling waters along the coast. Subsidence maintains a strong inversion that slopes down towards the coast where the BL flow is confined by the coastal mountains. The flow has been found to be close to supercritical over an extensive region (Dorman et al. 2000), and becomes supercritical as it rounds each cape and headland. Downwind of each cape an expansion fan forms, where the flow accelerates, and the BL collapses to form a very shallow stable layer. This study investigates the turbulence structure of the BL in and around such an expansion fan.

2. MEASUREMENTS

During June 1996 a series of 11 research flights were made by the NCAR C-130 Hercules off the coast of California as part of the Coastal Waves '96 field program (Rogers et al. 1998). This study uses data from a flight around Cape Mendocino on June 7. Turbulence data are sampled at 25Hz; mean quantities are calculated from 1-second averages. The three wind components are derived from pressure measurements around the radome; while aircraft motion was monitored by a combination of GPS and an inertial navigation system, and removed from the measured aircraft-relative winds. Temperature was measured by Rosemount platinum resistance thermometers and humidity by a lyman-alpha hygrometer.

The project focus on mesoscale flow structures and variability did not allow the extensive sets of straight and level flight legs at multiple levels usually used for turbulence measurements to be carried out; only 30m turbulence legs are available for most flights, from which surface fluxes are derived by eddy correlation. A large number of *sawtooth* profiles from ~15m to above the inversion were carried out; turbulence quantities have been derived from these following the approach of Tjernström (1993). Each profile is first carefully examined and the turbulent portion within the BL is selected. The selected portion is high-pass filtered to produce series of turbulent fluctuations about the altitude-dependent mean value. These series are multiplied together to produce series of instantaneous 2nd order moments. Finally block averaging produces profiles of the required turbulence quantities such as variances and fluxes. The final averaging length is carefully chosen to include all scales contributing to the fluxes – in this case 1km in the horizontal is sufficient; this corresponds to approximately 50m in the vertical. Note that the results of this process are individual estimates of turbulence quantities not statistically stable means. Tjernström (1993) normalized the turbulence profiles and then averaged multiple profiles to achieve

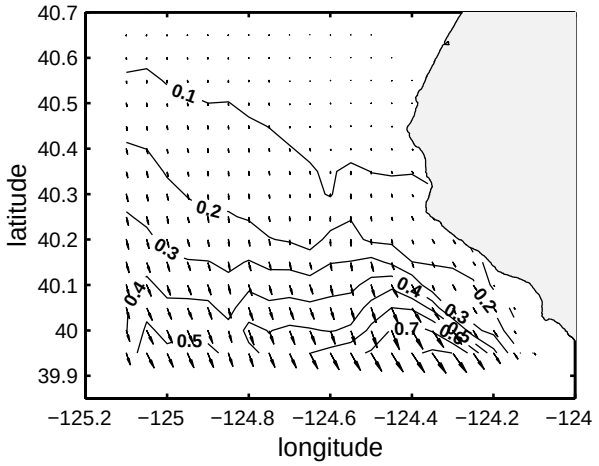

Figure 1. Surface wind stress (N m^{-2}) measured by eddy correlation from 30m flight legs.

**Corresponding author address:* Dr. Ian M. Brooks, Center for Coastal Studies, SIO-UCSD, 9500 Gilman Drive, La Jolla, CA. 92093-0209; email: ibrooks@ucsd.edu

profiles of mean fluxes; however the high degree of spatial variability observed in the present study makes such a process difficult, and we will consider only the individual profiles.

3. SURFACE FIELDS

Figure 1 shows the surface wind stress field derived from eddy correlation measurements at 30m. The curl of the wind stress has a maximum (of about 5×10^{-5} m s^{-2}) just downwind of the cape; this reinforces the coastal Ekman pumping and drives strong local upwelling, maintaining a pool of cold water south of the cape (Figure 2). Air moving over the cool coastal waters from offshore loses heat to the surface stabilizing the lower boundary layer. Figure 3 shows that a broad region, within about 40-50 km of the coast, becomes stably stratified; the maximum (negative) buoyancy flux is located roughly over the cold pool in the lee of the cape, though offset downwind, indicating the time required for the stable boundary layer to adjust to changes in surface conditions.

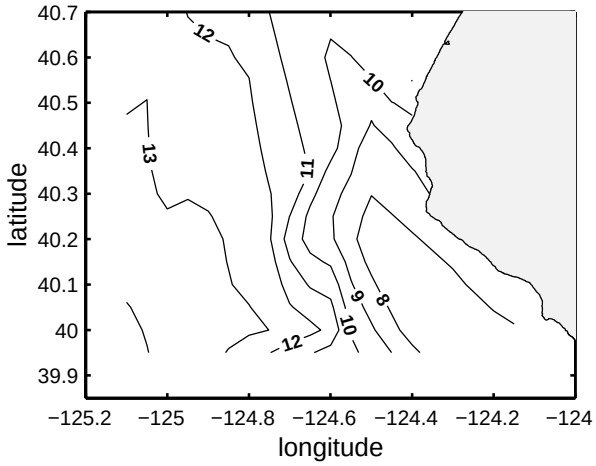

Figure 2. Sea surface temperature (°C).

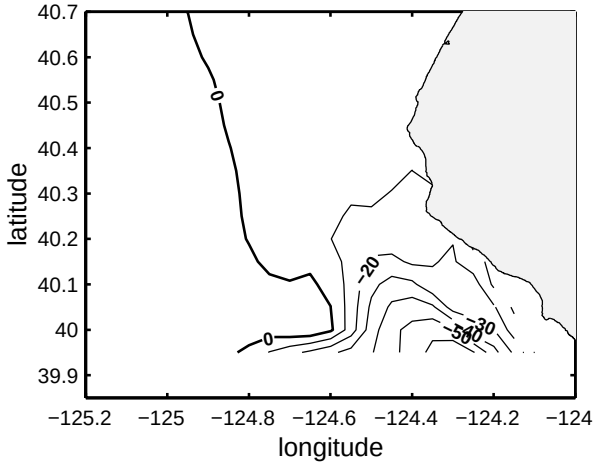

Figure 3. Surface buoyancy flux (W m^{-2}).

Bulk estimates of the surface fluxes have been calculated using the TOGA-COARE bulk flux algorithm (Fairall et al. 1996, Bradley et al. 2000). Figures 4, 5, and 6 show the difference between the bulk and directly measured wind stress, heat flux, and moisture flux. There are significant discrepancies throughout the coastal region. In the region of intense air-sea interaction south of Cape Mendocino the bulk parameterization greatly overestimates the downward fluxes of both sensible and latent heat. The discrepancies of 50 W m^{-2} or more would be expected to have a serious impact on the performance of regional numerical models, in particular of coupled ocean-atmosphere models. This could impair our ability to accurately forecast boundary layer depth, cloud cover, and fog formation along the coast, and would result in significant errors in the prediction of radar propagation conditions (Brooks 2001).

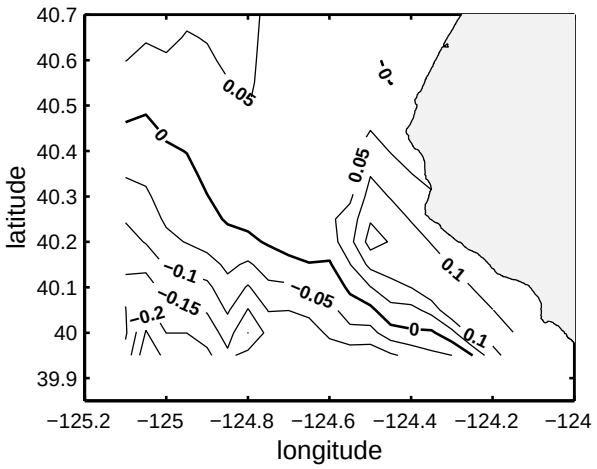

Figure 4. Discrepancy between the estimates of wind stress (N m^{-2})(bulk-eddy correlation)

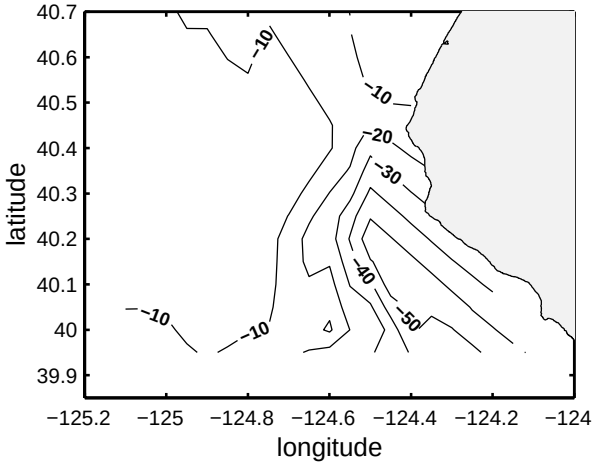

Figure 5. Discrepancy between estimates of the sensible heat flux (W m^{-2}) (bulk-eddy correlation)

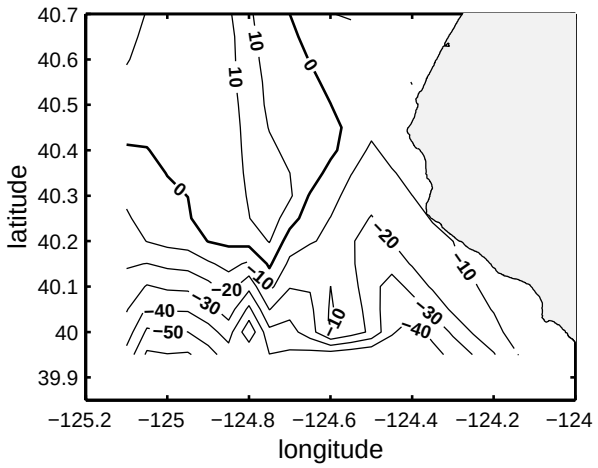

Figure 6. Discrepancy between estimates of the latent heat flux (W m^{-2}) (bulk-eddy correlation)

4. VERTICAL STRUCTURE

4.1 Mean and Turbulence Structure

Figure 7 shows the depth of the boundary layer, and illustrates the dramatic collapse in the lee of Cape Mendocino. The points A, B, and C are the locations of three individual aircraft profiles from which data are shown below. Figures 8 and 9 show profiles of the potential temperature and wind speed at A, B, and C. The two offshore profiles at A and B have a similar general structure. Both show evidence of a stable internal boundary layer (IBL) about 300 m deep – this forms when the marine air first moves over cooler water, and deepens as shear-driven turbulence entrains air into the layer. At A the IBL has only recently formed, decoupling the rest of the BL from the surface, and the main temperature inversion is still well defined. Further downwind, at B, the inversion has started to erode away. The wind speed profiles have a broad jet

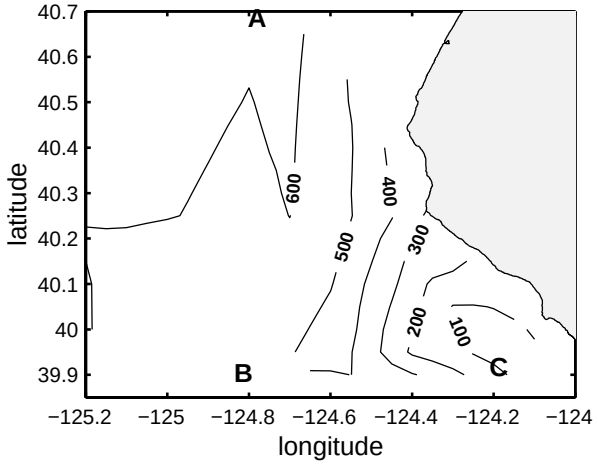

Figure 7. Boundary layer depth (m). The points A, B, C, mark the location of individual profiles discussed in the text.

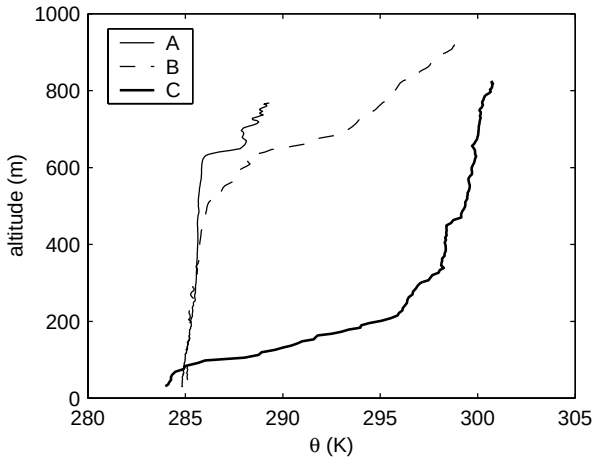

Figure 8. Profiles of potential temperature at A, B, and C.

structure with a maximum at the inversion. The wind speed increases with altitude from the surface throughout the IBL then remains almost constant up to the inversion, and decreases again above. A significant increase in mean wind speed takes place between A and B as the flow accelerates around the Cape. Turbulence is largely confined to the internal boundary layer (Figure 10), where shear at the surface is the primary generating mechanism. Wind shear across the main inversion, associated with the wind-speed jet, may also generate intermittent turbulence, resulting in entrainment and the erosion of the temperature inversion.

The profile at C, within the expansion fan, shows a very different structure. The temperature profile shows that the BL has collapsed to such an extent that it is effectively a deep inversion layer in contact with the surface. There is a pronounced wind-speed jet with a maximum at about 100 m, coincident with the maximum temperature gradient within the inversion. The strongest turbulence is confined below the jet maximum (Figure 11), but some weak turbulence is maintained well above

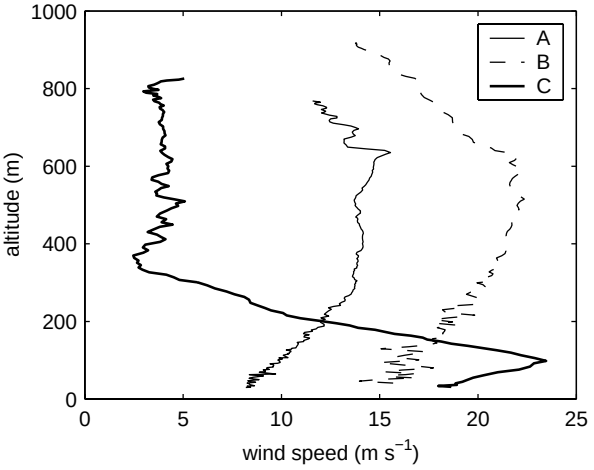

Figure 9. Profiles of mean wind speed at A, B, and C.

the collapsed boundary layer, driven by the wind shear. Strongly stable conditions inhibit vertical motion, and the horizontal velocity variances are 2–3 times greater than the vertical velocity variance for all the profiles.

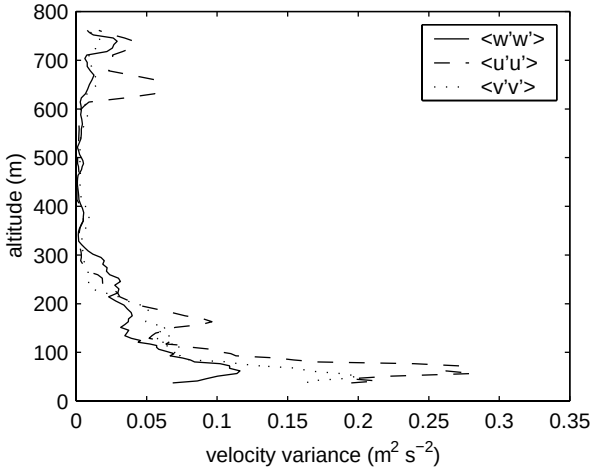

Figure 10. Profiles of *u*, *v*, and *w* velocity variances at A.

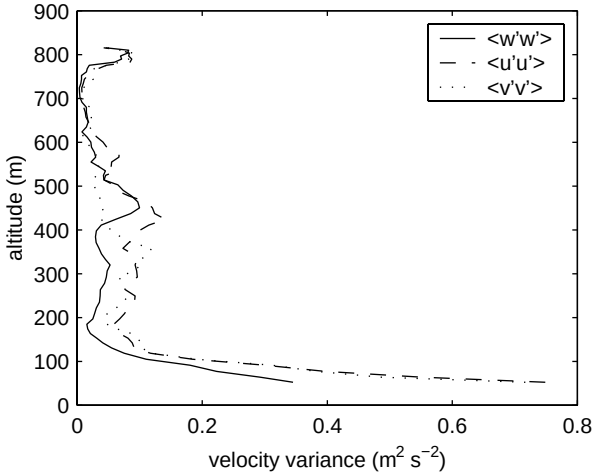

Figure 11. Profiles of *u*, *v*, and *w* velocity variances at C.

4.2 Local Similarity Scaling

There is no completely adequate theoretical framework to describe the turbulence structure of the stable boundary layer; and the spatially heterogeneous coastal environment presents a particularly challenging test for proposed schemes. Local similarity theory (Nieuwstadt 1984; Sorbjan 1986) presents a possible approach. It has been applied successfully in a number of studies of coastal boundary layers, primarily with offshore flow (Rogers et al. 1995; Tjerntröm and Smedman 1993; Brooks and Rogers 2000), and has been shown to apply in horizontally heterogeneous conditions (Shao and Hacker 1990). It has not yet, however, been determined whether local similarity provides a universally applicable description of turbulence under stable conditions.

Local similarity theory was first introduced by Nieuwstadt (1984), and extends the ideas of Monin-Obukhov surface similarity to the rest of the boundary layer by using local turbulence quantities as scaling parameters instead of their equivalent surface values. Nieuwstadt's theoretical study predicted that under stable conditions the scaled quantities approached constant values as z/L_L became large – in practice he found a constant value to be approached for z/L_L>~1. He confirmed the theory with tower-based observations of the nocturnal boundary layer. Subsequent studies have found results in broad agreement with Nieuwstadt's findings; a degree of scatter in the various reported values of scaled quantities has tended to be ignored. A small number of studies, however, have reported significantly different results; notably Shao and Hacker (1990) found that at least some scaled quantities increased in value with increasing z/L_L. Brooks and Rogers (2000) found that the scaled horizontal velocity variances were larger than those suggested by previous studies.

We will consider only the scaled standard deviation of vertical velocity here. Only data from within the continuously turbulent internal boundary layer is included in the analysis. Figure 12 shows profiles of the scaled standard deviation of vertical velocity within the turbulent IBL; according to Nieuwstadt (1984) these should approach a constant value of 1.4 under stable conditions, and be independent of altitude. The range of mean values observed by a number of previous studies is also indicated on the figure. It is clear that the scaled vertical velocities are broadly in agreement with previous findings. There is significant scatter in the individual values, but this is to be expected given the manner in which the estimates are derived from the

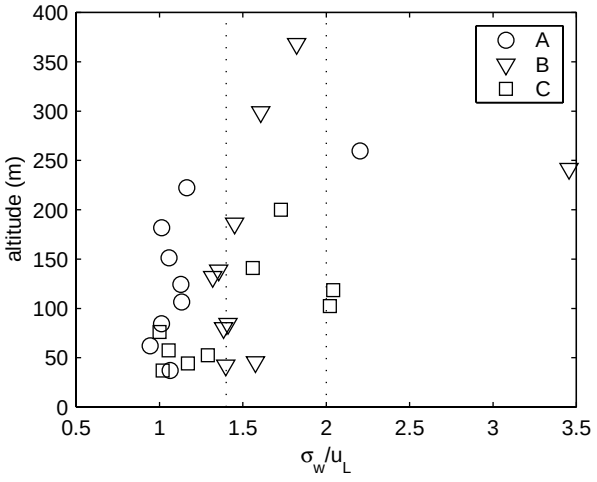

Figure 12. Profiles of scaled standard deviation of vertical velocity. In order to increase the number of data points available, profiles adjacent to those at A, B, and C have been included. The dotted lines indicate the range of values observed by previous studies.

aircraft profiles – indeed this makes the degree of ordering observed in the profiles quite remarkable. At A all but one of the values group very closely around a value of 1. At B the scaled values group close to 1.4, while at C the values are more scattered, but remain between the limits of 1-2. The profiles at B and C, however, suggest a trend of increasing value with altitude.

Figure 13 shows the scaled values of σ_w plotted against the stability parameter z/L_L for all the available profile data from June 7 (where L_L is a local Obukhov length). The individual estimates show considerable scatter, but when bin-averaged by stability show a well defined functional dependence on stability. This stability dependence explains much of the variability between locations and within profiles B and C observed in figure 12. Also shown is the fit obtained by Shao and Hacker (1990) and the constant value of 1.4 obtained by Nieuwstadt. Clearly the value approached at high

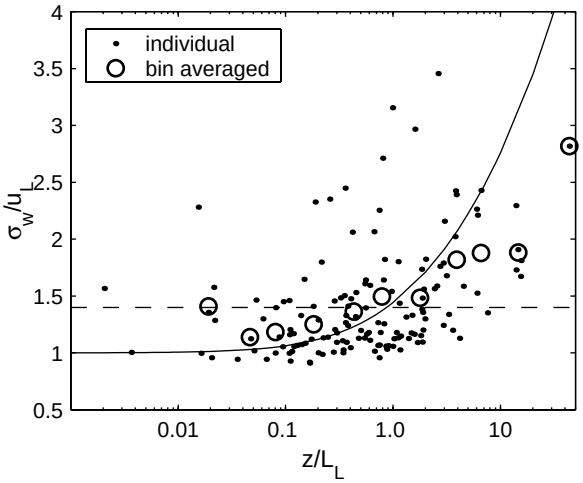

Figure 13. Scaled standard deviations of vertical velocity plotted against the stability parameter z/L_L for all the available profiles on June 7. Dots are individual estimates, circles are bin-averaged by stability. The solid line is the function found by Shao and Hacker (1990), the dashed line is the constant value of 1.4 suggested by Nieuwstadt (1984)

stability is greater than 1.4, but a lack of data makes it unclear if the value continues to increase, as found by Shao and Hacker, or if it approaches a constant close to 2. Further study with a more extensive data set is required.

Figure 14 shows the scaled values for each of the individual profiles within the expansion fan, along with the bin-averaged values for the entire data set. There is close agreement between the results from within the fan and the average over the entire data set. This is encouraging evidence for the applicability of local similarity theory in highly variable environments, where the local mean flow is strongly forced by external factors – in this case the interaction of the mesoscale flow and coastal topography.

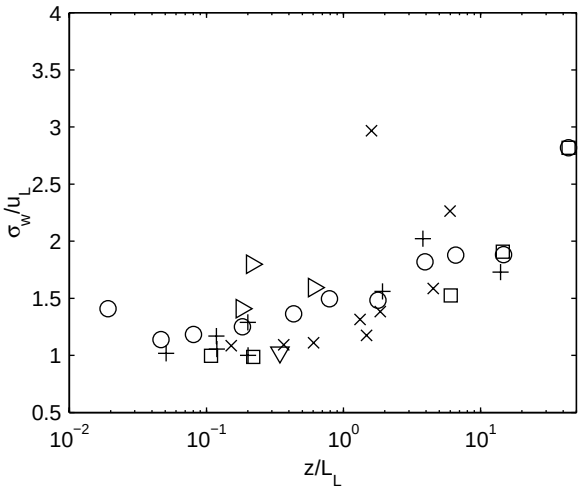

Figure 14. Scaled standard deviations of vertical velocity plotted against the stability parameter z/L_L. Circles are the bin-averaged results for all profiles. Other symbols are individual estimates from each profile within the expansion fan.

5. DISCUSSION

Aircraft measurements around Cape Mendocino have demonstrated the high degree of spatial variability in the surface fluxes in the coastal environment. Large discrepancies between the directly measured and parameterized fluxes were observed. It is unclear from the observations whether these arise purely from advective effects in a spatially variable environment, or if the form of the flux-profile relationships within the surface layer differ from those assumed by the parameterization. Advection is certainly expected to have a significant effect – Burk et al. (1999) found advection to play an important role in the turbulence kinetic energy budget in a modeling study of flow around an idealized cape based on CW96 conditions. Other recent studies have suggested that the assumed flux profile relationships may be invalid under some stable conditions, particularly where the latent heat flux is directed downwards, as is the case for much of the area studied here (Edson et al. 2000; Oost et al 2000). It seems likely that both may contribute to the failure of the bulk parameterization of the surface fluxes.

Local similarity theory has been found successful in scaling the vertical velocity within the stable internal boundary layer in spite of the strong external forcing on the flow. The scaling was found to apply equally to the collapsed boundary layer within the expansion fan and to the less strongly forced region upwind and away from the coast. This suggests that even in the highly heterogeneous coastal environment local turbulence statistics are controlled primarily by local turbulence processes rather than the external forcing.

The functional relationship between the scaled vertical velocity and stability differs from that suggested by the early studies of local similarity (Nieuwstadt 1994;

Sorbjan 1996). The small number of observations at the high stability precludes a firm conclusion about the form of the dependence – further studies will be conducted using the entire CW96 data set to address this issue, and examine other scaled quantities.

REFERENCES

Brooks, I. M., and D. P. Rogers, 2000: Aircraft observations of the mean and turbulent structure of a shallow boundary layer over the Persian Gulf. *Bound.-Layer Meteorol.*, **95**, 189-210.

Brooks, I. M. 2001: Air-sea interaction and the spatial variability of surface evaporation ducts in a coastal environment. *Geophys. Res. Letts.*, **28**, 10, 2009-2012.

Bradley, E. F., C. W. Fairall, J. E. Hare, and A. A. Grachev, 2000: An old and improved bulk algorithm for air-sea fluxes: COARE2.6A, *Preprints: 14th Symposium on Boundary Layers and Turbulence*, AMS Boston, 294-296.

Burk, S. D., T. Haack, and R. M. Samelson, 1999: Mesoscale simulation of supercritical, subcritical, and transcritical flow along coastal topography. *J. Atmos. Sci.*, **56**, 2780-2795.

Dorman, C. E., T. Holt, D. P. Rogers, and K. Edwards, 2000: Large scale structure of the June-July 1996 marine boundary layer along California and Oregon. *Mon. Wea. Rev.*, **128**, 1632-1652.

Edson, J. B., R. B. Beardsley, W. R. McGillis, J. E. Hare, and C. W. Fairall. 2000: Downward flux of moisture over the ocean. *Preprints 14th Symposium on Boundary Layers and Turbulence, AMS*, 511-515.

Fairall, C., E. F. Bradley, D. P. Rogers, J. B. Edson, and G. S. Young, 1996: Bulk parameterization of air-sea fluxes for the Tropical Ocean Global Atmosphere Coupled Ocean-Atmosphere Response Experiment. J. Geophys. Res., **101**, 3747-3764.

Nieuwstadt, F. T. M., 1984: The turbulent structure of the stable, nocturnal boundary layer, *J. Atmos. Sci.* **41**, 2202-2216.

Oost, W. A., C. M. J. Jacobs, and C. Van Oort, 2000: Stability effects on heat and moisture fluxes at sea. *Bound.-Layer Meteorol*, **95**, 271-302.

Rogers, D. P., Johnson, D. W., and Friehe, C. A., 1995: The stable internal boundary layer over a coastal sea. I: Airborne measurements of the mean and turbulence structure, *J. Atmos. Sci.*, **52**, 667-683.

Rogers, D. P., C. Dorman, K. Edwards, I. Brooks, K. Melville, S. Burk, W. T. Thompson, T. Holt, L. Ström, M. Tjernström, B. Grisogono, J. Bane, W. Nuss, B. Morley, and A. Schanot, 1998: Highlights of Coastal Waves 1996. *Bull. Amer. Meteorol. Soc.*,**79**, 1307-1326.

Shao, Y., and Hacker, J. M., 1990: Local similarity relationships in a horizontally inhomogeneous boundary layer, *Bound.-Layer. Met.*, **52**, 17-40.

Sorbjan, Z.., 1986: On similarity in the atmospheric boundary layer, *Bound.-Layer Meteor.*, **34**, 377-397.

Tjernström, M., 1993: Turbulence length scales in stably stratified free shear flow analyzed from slant aircraft profiles, *J. Appl. Met.*, **32**, 948-963.

Tjernström, M., and A.-S. Smedman, 1993: The vertical turbulence structure of the coastal marine atmospheric boundary layer. *J. Geophys. Res.*, **98,** (C3), 4809-4826.